© 2015. Published by The Company of Biologists Ltd | Development (2015) 142, 4288-4298 doi:10.1242/dev.115006

RESEARCH ARTICLE

Expression of an S phase-stabilized version of the CDK inhibitor Dacapo can alter endoreplication

Christina I. Swanson[1,*], Joy H. Meserve[2], Patrick C. McCarter[3], Alexis Thieme[4], Tony Mathew[4], Timothy C. Elston[3,5,6] and Robert J. Duronio[1,2,4,6,7,‡]

ABSTRACT

In developing organisms, divergence from the canonical cell division cycle is often necessary to ensure the proper growth, differentiation, and physiological function of a variety of tissues. An important example is endoreplication, in which endocycling cells alternate between G and S phase without intervening mitosis or cytokinesis, resulting in polyploidy. Although significantly different from the canonical cell cycle, endocycles use regulatory pathways that also function in diploid cells, particularly those involved in S phase entry and progression. A key S phase regulator is the Cyclin E-Cdk2 kinase, which must alternate between periods of high (S phase) and low (G phase) activity in order for endocycling cells to achieve repeated rounds of S phase and polyploidy. The mechanisms that drive these oscillations of Cyclin E-Cdk2 activity are not fully understood. Here, we show that the *Drosophila* Cyclin E-Cdk2 inhibitor Dacapo (Dap) is targeted for destruction during S phase via a PIP degron, contributing to oscillations of Dap protein accumulation during both mitotic cycles and endocycles. Expression of a PIP degron mutant Dap attenuates endocycle progression but does not obviously affect proliferating diploid cells. A mathematical model of the endocycle predicts that the rate of destruction of Dap during S phase modulates the endocycle by regulating the length of G phase. We propose from this model and our *in vivo* data that endo S phase-coupled destruction of Dap reduces the threshold of Cyclin E-Cdk2 activity necessary to trigger the subsequent G-S transition, thereby influencing endocycle oscillation frequency and the extent of polyploidy.

KEY WORDS: CRL4^{Cdt2}, CDK inhibitor, *Drosophila*, Cell cycle, Endocycle, Modeling, Polyploidy

INTRODUCTION

Developing organisms carefully regulate progression through the cell cycle to ensure proper tissue growth and differentiation. Most diploid cells proliferate by proceeding through the canonical $G_1 \rightarrow S \rightarrow G_2 \rightarrow M$ cell cycle. However, the cell cycle is remarkably malleable, and non-canonical cell cycles that omit gap phases, mitosis, or cytokinesis occur frequently in both plants and animals to support various developmental strategies and the biological functions of particular cells and tissues (Vidwans and Su, 2001). An important example is the endocycle, a cell cycle consisting of alternating periods of G and S phase without mitosis or cytokinesis resulting in polyploidy (Lee et al., 2009; Ullah et al., 2009b; De Veylder et al., 2011; Fox and Duronio, 2013; Zielke et al., 2013). Polyploid cells within otherwise diploid organisms (i.e. endopolyploidy) are widespread in nature, and well-studied examples include mammalian trophoblast giant cells, *Arabidopsis* trichome cells, and the cells of *Drosophila* ovaries and salivary glands. The biological purpose of endopolyploidy is poorly understood and probably varies widely depending on tissue function (Lee et al., 2009; Gentric and Desdouets, 2014). Examples of this breadth of function include the regulation of cell identity and differentiation (Hong et al., 2003; Raslova et al., 2007; Bramsiepe et al., 2010), accommodating tissue growth without disrupting epithelial integrity (Unhavaithaya and Orr-Weaver, 2012), and conferring resistance to DNA damage (Mehrotra et al., 2008; Ullah et al., 2008). In addition, polyploidy is increasingly implicated as a modulator of the development and progression of cancer (Storchova and Pellman, 2004; Davoli and de Lange, 2011; Fox and Duronio, 2013; Coward and Harding, 2014).

Endocycling cells utilize the same molecular toolkit as proliferating diploid cells, including cyclin-dependent kinases (CDKs), the transcriptional activator E2F, and the E3 ubiquitin ligase complexes APC/C and CRL4^{Cdt2} (Lee et al., 2009; Ullah et al., 2009b; De Veylder et al., 2011; Fox and Duronio, 2013; Zielke et al., 2013). Nevertheless, the role and/or regulation of these proteins can differ between canonical cycles and endocycles. For example, whereas multiple distinct CDKs govern progression through the canonical cell cycle, the endocycle is typically controlled by a single S phase CDK, such as the well-studied *Drosophila* Cyclin E-Cdk2 complex (Lilly and Duronio, 2005). A universal feature of S phase control is that replication origin licensing occurs only when CDK activity is low and origin firing occurs only when CDK activity is high (Arias and Walter, 2007; Diffley, 2011; Nordman and Orr-Weaver, 2012). Consequently, alternating periods of low (i.e. G phase) and high (i.e. S phase) Cyclin E-Cdk2 activity are required for repeated rounds of endocycle S phase (Follette et al., 1998; Weiss et al., 1998). The mechanisms that control oscillations of Cyclin E-Cdk2 activity in the *Drosophila* endocycle operate at many levels, including those that activate Cyclin E-Cdk2, such as the transcriptional induction of the *Cyclin E* gene by E2f1 (Duronio and O'Farrell, 1995), and those that inhibit Cyclin E-Cdk2, such as destruction of Cyclin E protein by the SCF^{Ago} E3 ubiquitin ligase (Moberg et al., 2001; Shcherbata et al., 2004; Zielke et al., 2011). Therefore, in order to fully understand the endocycle, all of the mechanisms that contribute to oscillations of Cyclin E-Cdk2 activity must be determined. Here, we

[1]Integrative Program for Biological and Genome Sciences, University of North Carolina, Chapel Hill, NC 27599, USA. [2]Curriculum in Genetics and Molecular Biology, University of North Carolina, Chapel Hill, NC 27599, USA. [3]Curriculum in Bioinformatics & Computational Biology, University of North Carolina, Chapel Hill, NC 27599, USA. [4]Department of Biology, University of North Carolina, Chapel Hill, NC 27599, USA. [5]Department of Pharmacology, University of North Carolina, Chapel Hill, NC 27599, USA. [6]Lineberger Comprehensive Cancer Center, University of North Carolina, Chapel Hill, NC 27599, USA. [7]Department of Genetics, University of North Carolina, Chapel Hill, NC 27599, USA.
*Present address: Biology Department, Arcadia University, Glenside, PA 19038, USA.

[‡]Author for correspondence (duronio@med.unc.edu)

Received 4 July 2014; Accepted 12 October 2015

Development (2015) 142, 4288-4298 doi:10.1242/dev.115006

investigate the role of regulated proteolysis of the CDK inhibitor (CKI) Dacapo (Dap) in the control of the *Drosophila* endocycle.

Dap is a member of the mammalian p21 family of CKIs and functions as a specific inhibitor of Cyclin E-Cdk2, often to promote exit from the cell cycle. In the embryonic epidermis, developing eye, and nervous system transcriptional induction of the *dap* gene causes rapid accumulation of Dap protein, resulting in inhibition of Cyclin E-Cdk2 activity and contributing to G1 cell cycle arrest (de Nooij et al., 1996; Lane et al., 1996; Firth and Baker, 2005; Buttitta et al., 2007; Escudero and Freeman, 2007; Sukhanova and Du, 2008; Colonques et al., 2011). However, in some tissues, Dap expression does not induce cell cycle arrest. In particular, Dap expression oscillates during endocycles of the polyploid nurse and follicle cells of the ovary (Hong et al., 2003, 2007). The mechanisms that generate these oscillations in expression are unknown, although cell cycle-linked post-translational regulation Dap has been proposed (Hong et al., 2003). Moreover, the functional role for oscillations of Dap expression in the endocycle is unclear. Importantly, Dap is required in both the nurse cells and follicle cells for normal endocycle progression. Endo S phase is prolonged in *dap* mutants (Hong et al., 2007), whereas Dap overexpression inhibits the endocycle (Weiss et al., 1998; Shcherbata et al., 2004; Zielke et al., 2011).

Here we show that Dap protein is destabilized during S phase by a motif called the PIP degron, which has been shown in other proteins to confer proteolysis via the $CRL4^{Cdt2}$ E3 ubiquitin ligase, a key regulator of both canonical cell cycles and endocycles (Abbas and Dutta, 2011; Zielke et al., 2011). $CRL4^{Cdt2}$ ubiquitylates substrates containing a PIP degron only after the PIP degron directly interacts with DNA-bound PCNA, the sliding clamp of the DNA replication machinery (Havens and Walter, 2009). As a result, $CRL4^{Cdt2}$ stimulates destruction of its substrates only when DNA is being replicated and PCNA is loaded onto DNA, such as during S phase or after DNA damage. $CRL4^{Cdt2}$ substrates play crucial roles in genome maintenance and include the replication licensing factor CDT1, the mammalian CKI p21 (also known as CDKN1A), the Set8 histone methyltransferase (also known as SETD8), and the *Drosophila* E2f1 transcription factor (Havens and Walter, 2011).

We found that mutation of the PIP degron results in inappropriate Dap accumulation during S phase, and that expression of a PIP-degron mutant Dap protein disrupts the normal periodicity of the endocycle, but does not affect proliferating cells or cell cycle exit. An *in silico* model of the endocycle recapitulates our results and suggests that endocycle frequency is directly influenced by the rate of Dap destruction during S phase. We propose that S phase-coupled Dap destruction is a common feature of the *Drosophila* endocycle and promotes the development of multiple tissues by modulating endocycle frequency.

RESULTS

Drosophila Dap contains a PIP degron necessary for S phase-coupled destruction

Dap, like several of its homologs, contains a putative PIP degron (Fig. 1A) (Havens and Walter, 2011). In addition, Dap protein stability is regulated by Cul4 (Higa et al., 2006), a member of the CRL4 complex. To determine if Dap is subject to S phase-coupled destruction, we used our previously developed flow cytometry assay to measure Dap accumulation during the cell cycle (Shibutani et al., 2008; Davidson and Duronio, 2011). In this assay, a GFP-Dap fusion protein is induced by a 30-min heat shock of S2 cells stably transfected with an *hsp70-GFP-dap* construct, and DNA content of the cell population is determined by flow cytometry at different times after induction (Fig. 1B,C). In these populations, not all of the cells express GFP-Dap, allowing us to determine in which phase of the cell cycle GFP-Dap accumulates by comparing DNA content in GFP+ cells to that of all the cells in the population. Two hours following heat shock, GFP-Dap accumulated in cells in G1, S, and G2. However, a smaller percentage of GFP+ cells had S phase DNA content compared with the whole population (Fig. 1B,C). Because the *hsp70* promoter drives GFP-Dap transcription, and the mRNA produced by these transgenes contains minimal 3′UTR sequences, this difference most likely arises from S phase-specific post-translational regulation rather than transcriptional or translational controls. Moreover, GFP protein is stable in S phase cells (Shibutani et al., 2008; Davidson and Duronio, 2012).

To test if the regulation of Dap protein accumulation involves the PIP degron, we generated three different alanine-substitution mutations that changed either all consensus PIP degron residues (mDeg), only the residues predicted to contact PCNA (mPIP), or only a lysine residue predicted to contact the Cdt2 subunit of $CRL4^{Cdt2}$ (mK+4) (Fig. 1A) (Havens and Walter, 2011). All three PIP degron mutant proteins accumulated throughout the cell cycle with no significant difference between the percentage of GFP+ cells in S phase and the whole population (Fig. 1B,C). At four hours after induction of GFP-Dap^{mDeg} expression, we observed an increase in the number of G1 cells in the GFP+ population relative to the whole population, as predicted by inhibition of Cyclin E-Cdk2 activity (Fig. S1A). This result suggests that the mDeg mutation did not disrupt the CDK inhibitory function of Dap. We did not perform a similar experiment with the other two PIP degron mutant alleles, as they each change only a subset of the residues mutated in the mDeg allele and therefore will probably also retain CKI function. We conclude from these data that the *Drosophila* Dap protein is subject to PIP degron-dependent, S phase-coupled destruction.

To examine S phase stability of Dap *in vivo*, we stained BrdU-labeled embryos with anti-Dap antibodies and observed that the endogenous Dap protein did not accumulate to high levels in S phase nuclei (Fig. 1D). While this observation is consistent with S phase-coupled destruction of the Dap protein, it could also reflect cell cycle-specific transcriptional regulation of Dap expression. Therefore, we also used the GAL4/UAS system to express GFP-Dap or GFP-Dap^{mDeg} transgenes under the control of a UASp promoter, which would bypass any cell cycle-specific transcriptional regulation of the endogenous gene. When expressed ubiquitously using a *tub-GAL4* driver, GFP-Dap levels were much lower in replicating nuclei compared with nuclei that were not replicating or replicating nuclei expressing only GFP (Fig. 1E,F,H; Fig. S1B). By contrast, GFP-Dap^{mDeg} accumulated in BrdU-positive nuclei (Fig. 1G,H; Fig. S1B). GFP-Dap^{mDeg} was significantly more stable in replicating nuclei than GFP-Dap, indicating that mutation of the PIP degron stabilized the GFP-Dap^{mDeg} protein in S phase. We conclude from these data that the PIP degron of Dap contributes to S phase-coupled destruction.

S phase stabilization of Dap does not disrupt mitotic cell cycles

We next investigated the *in vivo* function of PIP-degron regulation of Dap by comparing the developmental and cell cycle phenotypes after expression of wild-type and PIP degron mutant GFP-Dap proteins. During gastrulation, *Drosophila* embryonic epidermal cells perform three cell division cycles before arresting in G1 of the seventeenth cell cycle. Induction of zygotic Dap transcription during interphase of cycle 16 is required for this cell cycle arrest (de Nooij et al., 1996; Lane et al., 1996). We hypothesized that PIP

Development (2015) 142, 4288-4298 doi:10.1242/dev.115006

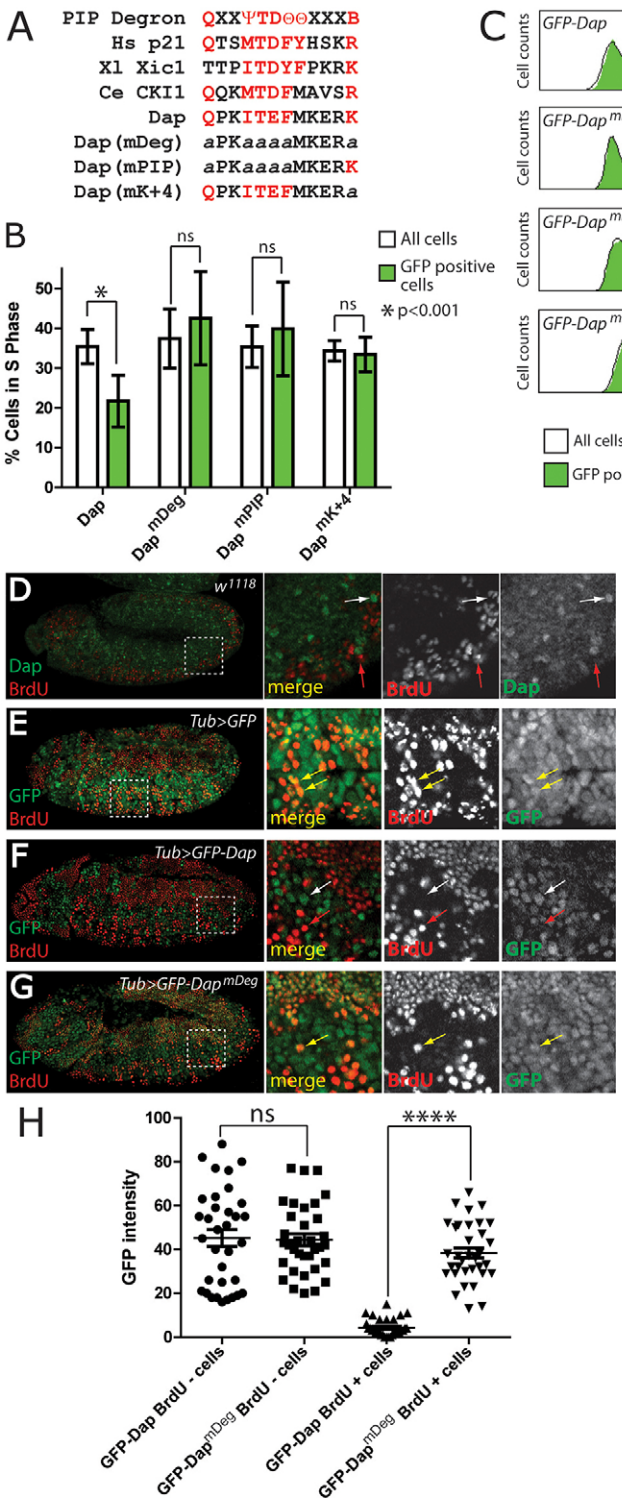

Fig. 1. Dap contains a PIP degron that mediates S phase-coupled destruction. (A) Alignment of human (Hs) p21, *Xenopus* (Xl) Xic1, *C. elegans* (Ce) CKI-1, and Dap PIP degrons. PCNA- and Cdt2-binding residues highlighted in red; consensus PIP degron at top. The alanine substitution mutations in the Dap PIP degron are italicized. (B,C) Flow cytometry of *hsp70-GFP-Dap* cells analyzed 2 h after 30-min heat shock. (B) The percentage of GFP-positive cells in S phase (green bars) is plotted with the percentage of cells in the total population in S phase (white bars; includes GFP-positive and GFP-negative cells). Error bars indicate standard deviation (s.d.), **P*<0.05. (C) Representative cell cycle profiles with solid traces indicating the total cell population and green traces indicating GFP-positive cells. (D) 7-h-old wild-type embryo stained with anti-Dap antibodies (green) and BrdU (red). White arrows indicate a BrdU-negative cell with high Dap expression, red arrows indicate a BrdU-positive cell with low Dap expression. White box outlines area shown in higher magnification. (E-G) 5-h-old embryos expressing GFP, GFP-Dap, or GFP-Dap^{mDeg} using *tub-Gal4* and stained with anti-GFP antibodies (green) and BrdU (red). Yellow arrows in E,G indicate GFP-positive cells that are also BrdU positive, white and red arrows in F as in D. Note that GFP-Dap^{mDeg} accumulates in cells undergoing S phase (G). (H) Quantification of GFP fluorescence in BrdU-negative (left) and BrdU-postive (right) cells from 5-h-old *tub>GFP-Dap* and *tub>GFP-Dap*^{mDeg} embryos. Each point represents a single cell; three embryos per genotype were used for quantification. Middle bars represent mean; error bars indicate s.d.; ns, not significant; *****P*<0.00005.

degron-mediated destruction during S phase of cycle 16 might function to prevent premature accumulation of Dap and precocious cell cycle arrest. In contrast to our expectations, embryonic epidermal cells expressing S phase-stabilized GFP-Dap^{mDeg} progress normally through S phase of cell cycle 16, as do cells expressing either GFP or GFP-Dap (Fig. 2A-C). After germ band retraction, cells expressing GFP-Dap or GFP-Dap^{mDeg} under the control of *prd-GAL4* are similar in size to neighboring control cells that do not express these proteins, indicating that they have undergone the same number of cell divisions and arrest normally in G1 of cycle 17 (Fig. 2D,E). These results differ from previously published experiments in which overexpression of Dap in the embryonic epidermis using a *UASt-Dap* transgene induces premature cell cycle arrest (Lane et al., 1996). We suspected that this discrepancy results from the UASt promoter driving higher levels of expression than our *UASp-Dap* transgenes. We confirmed this suspicion by western blotting of embryo extracts (Fig. S2A), and also replicated the Lane et al. (1996) data using a *UASt-Dap*

Development (2015) 142, 4288-4298 doi:10.1242/dev.115006

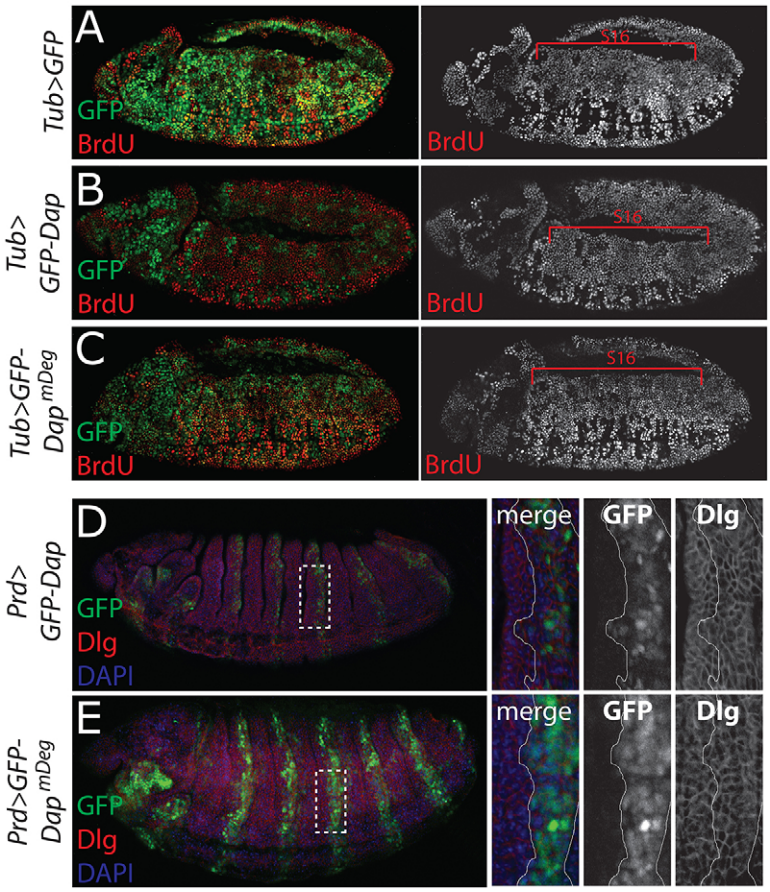

Fig. 2. S phase-stabilized Dap expression does not disrupt the embryonic epidermal cell cycle program. (A-C) 6-h-old embryos expressing GFP (A) or GFP-Dap (B,C) transgenes with *tub-Gal4* and stained for GFP (green) and BrdU (red). Epidermal cells in all three genotypes enter and progress normally through S phase of cell cycle 16 (S16). (D,E) Germ band-retracted embryos expressing GFP (D) or Dap (E) transgenes with *prd-Gal4* and stained with anti-GFP (green) and anti-Dlg (red) antibodies to mark the cell cortex to indicate cell size. White boxes outline area shown in higher magnification.

transgene (Fig. S2B,C). We also found no overt differences in either the proliferation or differentiation of cells in the central and peripheral nervous systems in embryos ubiquitously expressing either GFP-Dap or GFP-Dap^{mDeg} (Fig. S3). Finally, expression of the wild-type or S phase-stabilized Dap using *engrailed-GAL4* did not disrupt growth or proliferation in the posterior compartment of third instar larvae wing imaginal discs (Fig. S4). We conclude that the increase in Dap protein accumulation during S phase resulting from mutation of the PIP degron is insufficient to significantly disrupt cell cycle progression or exit in these tissues.

Expression of Dap^{mDeg} disrupts the pattern of endocycle S phase in the embryonic midgut

Although S phase-coupled destruction of Dap did not overtly affect the mitotically active tissues we examined, we found that *tub>GFP-Dap^{mDeg}* progeny do not survive to adulthood. Approximately 90% of *tub>GFP-Dap^{mDeg}* embryos fail to hatch, unlike *tub>GFP-Dap* embryos, which hatch at normal rates and survive to adulthood. To determine whether GFP-Dap^{mDeg} expression affected cell cycle progression, we performed BrdU labeling of *tub>GFP-Dap^{mDeg}* embryos, where we observed a phenotype in the developing alimentary tract. The cells of the midgut and hindgut normally become polyploid and begin endocycling in Stage 13 of embryogenesis. In Stage 13 *tub>GFP* control embryos, cells throughout the anterior and posterior midgut enter the first endocycle S phase simultaneously (Fig. 3A). Midgut BrdU incorporation in Stage 13 *tub>GFP-Dap* embryos is similar to controls (Fig. 3B,D). By contrast, BrdU incorporation is scattered irregularly in the midgut of Stage 13 *tub>GFP-Dap^{mDeg}* embryos (Fig. 3C). Quantification of this phenotype revealed a reduced midgut S phase index without a change in the number of midgut cells (Fig. 3D,E), suggesting an endocycle defect rather than an earlier arrest of cell proliferation.

S phase-coupled destruction of Dap can modulate normal endocycle progression

To further investigate whether S phase-coupled destruction of Dap has a role in endocycling tissues, we examined follicle cells of the developing ovary because previous studies reported that Dap expression fluctuates in these cells and that Dap function is required for normal follicle cell endocycles (Hong et al., 2003, 2007). We suspected that PIP degron-mediated destruction might contribute to both the observed fluctuations in Dap protein accumulation and normal endocycle progression within the follicle cells.

We tested this hypothesis by expressing our Dap transgenes in endocycling follicle cells using the *c323-GAL4* driver, which activates follicle cell-specific expression beginning in Stage 8 egg chambers (Manseau et al., 1997). Whereas GFP accumulated uniformly in all follicle cells at Stage 9 (Fig. 4A), GFP-Dap accumulated only in non-replicating cells (Fig. 4B,D,F; Fig. S1C). In contrast to GFP-Dap, GFP-Dap^{mDeg} accumulated in both EdU-positive and EdU-negative follicle cells (Fig. 4C,E,F; Fig. S1C). GFP-Dap^{mDeg} was significantly more stable in EdU-positive cells than GFP-Dap, indicating that PIP-degron-mediated S phase destruction contributes to oscillating levels of Dap expression in endocycling follicle cells (Fig. 4F). Interestingly, unlike GFP, GFP-Dap^{mDeg} accumulation was not uniform: some follicle cells with significant EdU incorporation had low levels of GFP-Dap^{mDeg} accumulation (Fig. 4E,F; Fig. S1C), suggesting an additional, PIP degron-independent mode of Dap turnover that is itself linked to

Development (2015) 142, 4288-4298 doi:10.1242/dev.115006

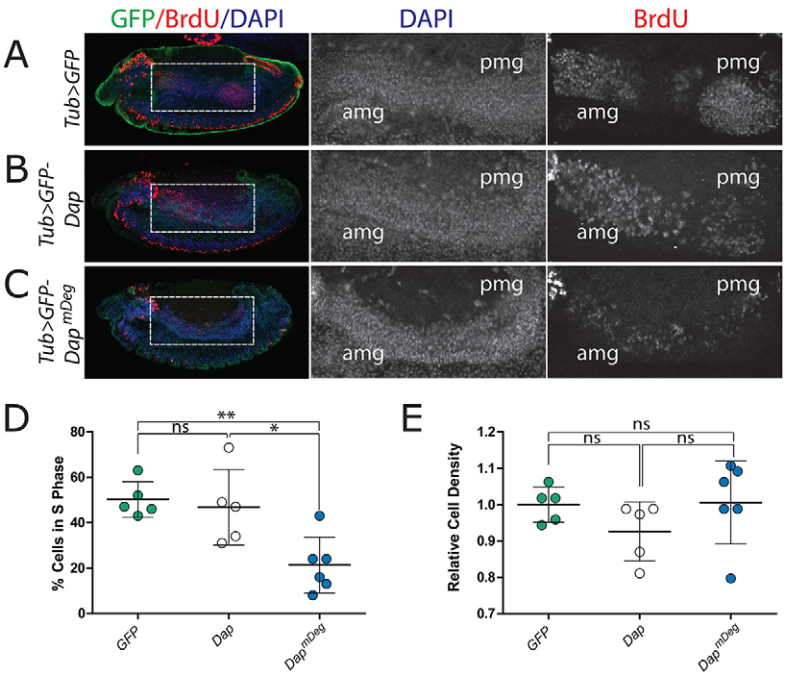

Fig. 3. S phase-stabilized Dap expression disrupts endocycle progression in the embryonic gut. (A-C) Stage 13 embryos expressing GFP (A) or GFP-Dap (B,C) transgenes with *tub-Gal4* and stained for GFP (green) and BrdU (red). The first endocycle S phase in the anterior midgut (amg) and posterior midgut (pmg) normally occurs concurrently. (D) Quantification of percentage of anterior midgut cells undergoing S phase in Stage 13 embryos. (E) Relative cell density in the anterior midguts of Stage 13 embryos. Each dot represents one embryo. Middle bars represent mean; error bars indicate s.d.; ns, not significant; **P*<0.05; ***P*<0.005.

either replication or Cyclin E-Cdk2 activity during S phase (see Discussion). We also noted that GFP-Dap^{mDeg} accumulated to greater levels than GFP-Dap outside of S phase as well; because these transgenes are under the same transcriptional controls, differences in expression must arise from differences in PIP degron-regulated protein stability and/or resulting changes to the endocycle (i.e. prolonged G phase or arrest) (Fig. 4F, Fig. S1C).

We assessed the effect of Dap transgene expression on endocycle progression by calculating the percentage of follicle cells undergoing S phase in Stage 9 egg chambers by EdU labeling. We found that an average of 38% of GFP-expressing control follicle cells were in S phase at this stage (Fig. 4G). Expression of GFP-Dap resulted in a small but statistically significant decrease in the number of S phase cells (27%) (Fig. 4G). Expression of GFP-Dap^{mDeg}, however, resulted in a sharp decline in the percentage of follicle cells undergoing S phase (11%) (Fig. 4G). Thus, expression of wild-type Dap, which is rapidly destroyed during S phase, is well tolerated by follicle cells, whereas expression of a version of Dap that is less efficiently destroyed during S phase impairs endocycle progression. Follicle cells perform 3 endocycles over a 24-h period between Stages 7 and 9 (Calvi et al., 1998). Thus, between Stages 8 and 9 only one to two endocycles occur, suggesting that follicle cell endocycle disruption occurs relatively soon after GFP-Dap^{mDeg} expression.

To extend these observations, we examined the highly polyploid *Drosophila* salivary gland cells, which are frequently used as a paradigm to dissect mechanisms of endocycle progression. Previous work showed that Dap is not absolutely required for salivary gland endocycles, but that the average size and DNA content of *dap* mutant salivary glands is slightly reduced relative to wild type (Zielke et al., 2011). We detected low levels of endogenous Dap protein in salivary glands that oscillate in a pattern reminiscent of that in the follicle cells: Dap accumulation is highest in G phase nuclei and lowest or absent in replicating nuclei (Fig. 5A). Using the *ptc>GAL4* driver, we found that GFP-Dap is absent from cells undergoing S phase and highest in cells that are not replicating (Fig. 5C,E,H; Fig. S1D). We also detected cells that were not replicating and lacked GFP-Dap (Fig. 5C,E), perhaps representing cells that have stopped endocycling. By contrast, Dap^{mDeg} is significantly more stable in S phase nuclei than Dap (Fig. 5D,F,H; Fig. S1D). As in follicle cells, the stabilization of Dap^{mDeg} was not uniform in all EdU-positive cells in the salivary gland, suggesting that PIP-degron-independent mechanisms also control Dap stability in these cells (Fig. 5D,F,H; Fig. S1D).

As before, we assessed endocycle progression by calculating the percentage of cells undergoing S phase after Dap expression. While expression of GFP-Dap did not significantly alter the percentage of S phase cells in the salivary gland compared with GFP-only controls (33% vs 42%, respectively), expression of Dap^{mDeg} resulted in a dramatic decline in the percentage of S phase cells (7%) (Fig. 5I). Furthermore, nuclear size and DAPI intensity were significantly lower in glands expressing Dap^{mDeg} (Fig. 5J,K), indicating a reduction in endocycle frequency that prevents cells from reaching normal ploidy. Western blotting indicated that GFP-Dap and GFP-Dap^{mDeg} were overexpressed in salivary glands to similar levels (Fig. 5G). Thus, although Dap is not required for the salivary gland endocycle to proceed, we propose that PIP-degron-mediated regulation of Dap accumulation in this tissue might contribute to normal endocycle progression.

Mathematical modeling predicts that S phase-coupled Dap destruction modulates endocycle oscillations

Our data indicate that Dap undergoes S phase-coupled destruction in multiple tissues. Whereas expression of wild-type Dap using UASp is well tolerated by the cell types we examined, a decline in cells undergoing endo S phase results when Dap^{mDeg} is expressed (Fig. 3D, Fig. 4G, Fig. 5I). This phenotype suggests that the endocycle is particularly sensitive to changes in S phase-coupled destruction of Dap. One possible explanation for these results is that a failure to fully destroy Dap during S phase might increase the amount of Cyclin E-Cdk2 needed to trigger the G-S transition in the subsequent endocycle. If true, then the amount of time required to achieve the critical level of Cyclin E-Cdk2 activity might also

Development (2015) 142, 4288-4298 doi:10.1242/dev.115006

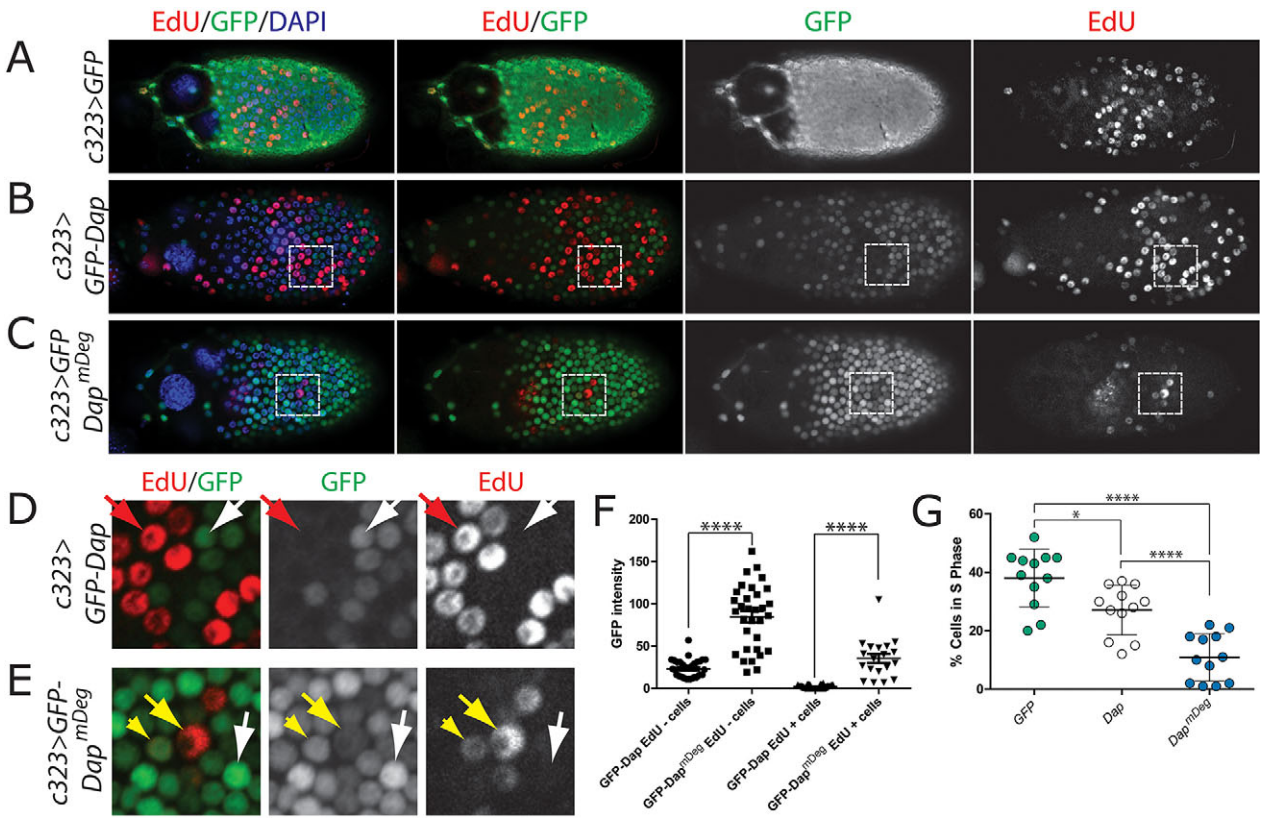

Fig. 4. S phase-stabilized Dap expression disrupts endocycle progression in ovarian follicle cells. (A-C) Stage 9 egg chambers expressing GFP (A) or GFP-Dap (B,C) transgenes with *c323-GAL4* and stained for GFP (green), EdU (red), and DAPI (blue). (D,E) Higher magnification views (white boxes in B and C, respectively) of EdU-negative nuclei with high GFP-Dap or GFP-Dap^{mDeg} (white arrows), an EdU-positive nucleus with low GFP-Dap expression (red arrows), and EdU-positive nuclei with different amounts of GFP-Dap^{mDeg} (yellow arrows/arrowheads). Nuclei with extensive EdU incorporation (yellow arrow) typically had less GFP-Dap^{mDeg} than nuclei with more modest EdU incorporation (yellow arrowhead). (F) Quantification of GFP fluorescence in EdU-negative (left) and EdU-postive (right) cells from Stage 10 ovarian follicle cells. Each point represents a single cell; three egg chambers per genotype were used for quantification. (G) Quantification of the percentage of follicle cells undergoing S phase in Stage 10 egg chambers. Each dot represents one egg chamber. Middle bars represent mean; error bars indicate s.d.; *P<0.05; ****P<0.00005.

increase, resulting in a reduction of endocycle oscillation frequency. We tested this hypothesis using a previously described mathematical model of the *Drosophila* endocycle (Zielke et al., 2011). This original model did not include any input from Dap protein. Based on our results, we modified the model to incorporate both Dap expression and S phase-coupled Dap destruction (Fig. 6A). We reasoned that this new model would more accurately reflect the *Drosophila* endocycle program and provide insight into how changing the rate of Dap destruction during S phase would affect endocycle oscillation.

The new model incorporates three key regulatory relationships between Dap and Cyclin E-Cdk2 activity: (i) transcriptional activation of Dap by Cyclin E, described previously (de Nooij et al., 2000); (ii) direct inhibition of Cyclin E-Cdk2 activity by Dap; and (iii) destruction of Dap triggered by CRL4^{Cdt2} after Cyclin E synthesis promotes S phase entry (Fig. 6A). Also, we used model rate parameters that recapitulated the subtle changes in endocycle frequency observed in *dap* mutants (Zielke et al., 2011) (Table S1). We examined several scenarios with this model. First, the addition of Dap to the original model (Fig. 6B) reduces the frequency of Cyclin E oscillations by lengthening G phase (i.e. E2F spike duration), thereby altering endocycle periodicity (Fig. 6C). Second, removal of S phase-coupled destruction (i.e. CRL4 in the model) of endogenous Dap results in the elimination of endocycle oscillations (Fig. 6D).

We next modeled our transgenic system of exogenous, continuously expressed Dap. At low levels of expression, exogenous Dap affects the periodicity of the endocycle by slightly decreasing the frequency of Cyclin E oscillations and slightly increasing G phase length (Fig. 6E compared with 6C). This change is consistent with our *in vivo* observation that *UASp-Dap* expression reduces the number of S phase follicle cells even with PIP-degron regulation intact (Fig. 4F). Further increasing the level of exogenous Dap expression further diminishes the oscillation frequency of the endocycle (Fig. 6G). When S phase-coupled destruction of exogenous Dap is eliminated there is a rapid cessation of endocycle oscillations (Fig. 6F,H), consistent with our *in vivo* observations in both follicle cells and salivary glands that Dap^{mDeg} expression reduces the number of cells in S phase. Finally, because we noted that mutation of the PIP degron did not completely stabilize Dap during S phase in the follicle cells and salivary glands, we modeled incomplete degradation of endogenous Dap to examine how CRL4^{Cdt2} might function cooperatively with other mechanisms to regulate Dap stability and endocycle progression. Strikingly, even a modest reduction in the rate of Dap destruction doubles the length of G phase (Fig. 6I). In fact, in our model, partial stabilization of endogenous Dap has a more dramatic effect on the endocycle than overexpression of a version of Dap that is still subject to S phase destruction (Fig. 6E,I). Thus, mathematical modeling supports our *in vivo* observations that the endocycle is sensitive to expression of a

Development (2015) 142, 4288-4298 doi:10.1242/dev.115006

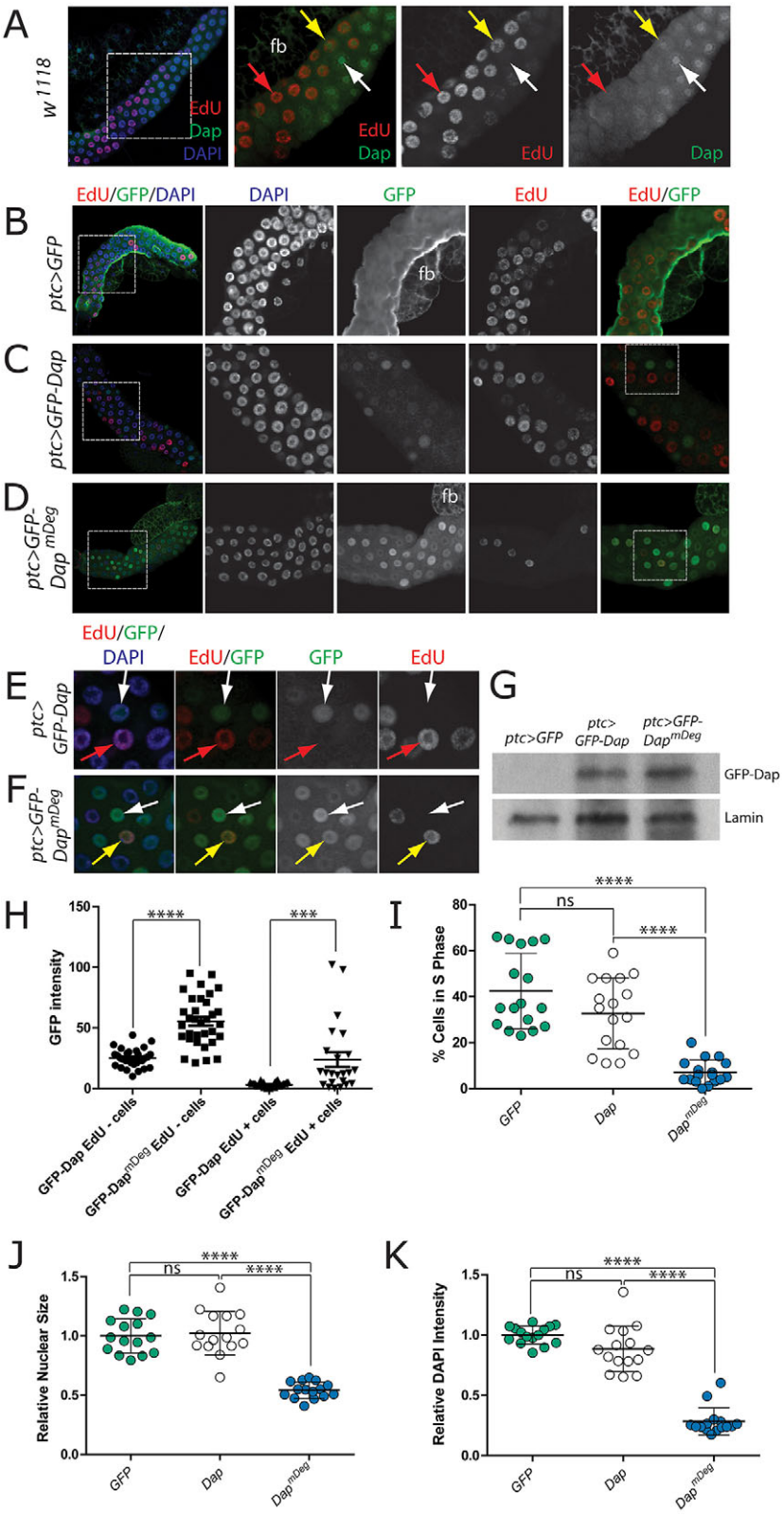

Fig. 5. S phase-stabilized Dap expression disrupts endocycle progression in salivary glands. (A) Wild-type third instar larval salivary gland stained with anti-Dap antibodies (green), DAPI (blue) and EdU (red). White box outlines the higher magnification region showing an EdU-negative, G phase nucleus with high levels of Dap (white arrow), an extensively labeled S phase nucleus with no Dap (red arrow), and an S phase nucleus with a low level of Dap protein that does not overlap with the EdU signal (yellow arrow). (B-D) Early third instar larval salivary glands expressing GFP (B) or GFP-Dap transgenes (C,D) with *ptc-GAL4* and stained for GFP (green), DAPI (blue) and EdU (red). fb, fat body. (E,F) Higher magnification images of *ptc>GFP-Dap* and *ptc>Dap*^{mDeg} salivary glands (white boxes in right panels of C,D) showing EdU-negative nuclei with high GFP-Dap or GFP-Dap^{mDeg} (white arrows), an EdU-positive nucleus with very low or no GFP-Dap (red arrow), and an EdU-positive nucleus with high GFP-Dap^{mDeg} (yellow arrow). (G) Immunoblot of equal numbers of salivary glands of the indicated genotypes using anti-GFP antibodies to detect GFP-Dap. Anti-lamin is a loading control. (H) Quantification of GFP fluorescence in EdU-negative (left) and EdU-postive (right) cells from salivary glands. Each point represents a single cell; three glands per genotype were used for quantification. (I-K) Quantification of the S phase index (I), nuclear size (J), and DAPI intensity (K) in salivary glands expressing GFP or GFP-Dap transgenes. In J and K *ptc>GFP-Dap* and *ptc>GFP-Dap*^{mDeg} measurements were normalized to the average nuclear size and DAPI intensity in *ptc>GFP* glands, respectively. Middle bars indicate the mean; error bars indicate s.d.; ns, not significant; ***P<0.0005; ****P<0.00005.

PIP-degron mutant Dap and suggests that S phase-coupled destruction of Dap modulates endocycle progression.

DISCUSSION

In this study we show that the Cyclin E-Cdk2 inhibitor Dap contains a PIP degron that confers destruction of Dap protein during S phase in multiple tissues during *Drosophila* development. Thus far, all proteins with a functional PIP degron are substrates of CRL4^{Cdt2}, making it highly probable that Dap destruction is mediated by the CRL4^{Cdt2} E3 ubiquitin ligase. CRL4^{Cdt2} regulation of the Cip/Kip family of CKIs is highly conserved: *Xenopus* Xic1 (also known as Cdknx), *C. elegans* CKI-1, and human p21 all are targets of

Development (2015) 142, 4288-4298 doi:10.1242/dev.115006

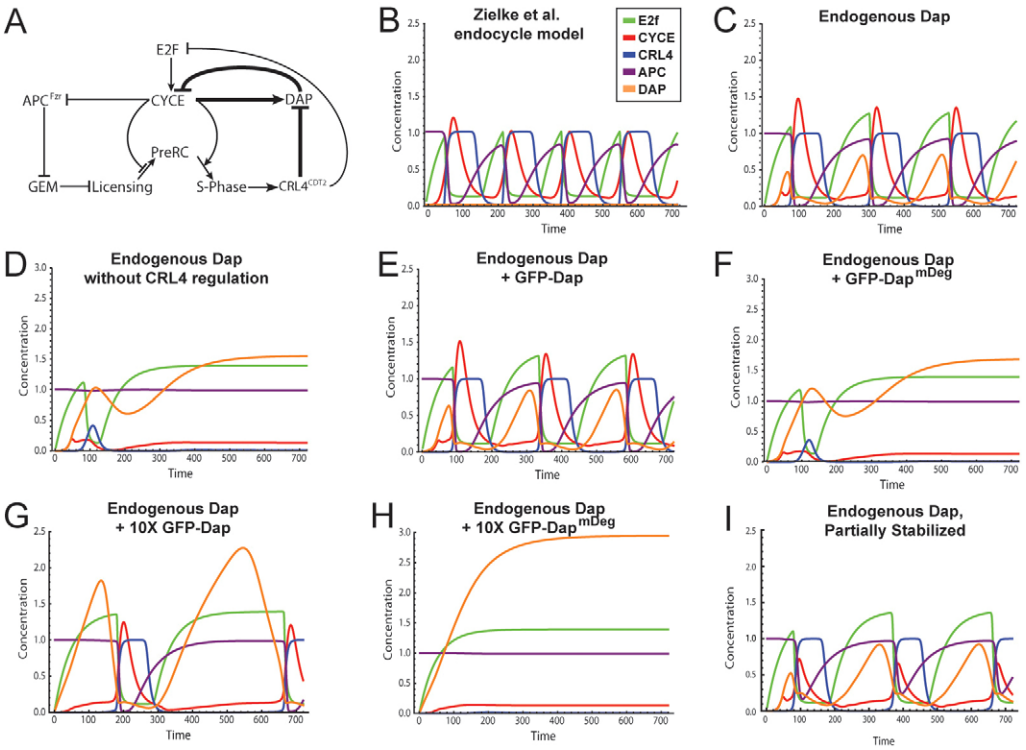

Fig. 6. Mathematical modeling of the *Drosophila* endocycle. (A) Network diagram of the molecular interactions within an existing endocycle model (Zielke et al., 2011). Our additions to the previous model are in bold. (B) The Zielke et al., (2011) endocycle model, which did not include Dap, showing oscillation of the levels or activity of key cell cycle regulators. The *x* and *y* axes display arbitrary units. (C) The revised endocycle model including Dap (orange curves). (D) Removal of $CRL4^{Cdt2}$ regulation of endogenous Dap eliminates endocycle oscillations. (E-H) Modeling exogenous Dap. Addition of wild-type, exogenous Dap at either 1× (E) or 10× (G) relative levels reduces endocycle frequency. Removal of $CRL4^{Cdt2}$ regulation of exogenous Dap at either level of expression (F and H, respectively) eliminates endocycle oscillations. (I) Reduction of S phase degradation of endogenous Dap alters endocycle periodicity.

$CRL4^{Cdt2}$ (Abbas et al., 2008; Kim et al., 2008, 2010; Nishitani et al., 2008). Yet relatively little is known about the *in vivo* developmental function of $CRL4^{Cdt2}$-mediated destruction of CKIs. In studies of *cul-4* and *cdt-2* RNAi-treated *C. elegans*, S phase stabilization of CKI-1 inhibited nuclear export of the replication licensing factor CDC-6 and contributed to re-replication, a function that appears to be conserved for mammalian p21 (Kim et al., 2007, 2008). Interpreting phenotypes resulting from $CRL4^{Cdt2}$ depletion is complicated because $CRL4^{Cdt2}$ has multiple substrates, including those such as Cdt1 that function in DNA replication (Hu et al., 2004; Arias and Walter, 2006; Hu and Xiong, 2006; Senga et al., 2006). By mutating the PIP degron, we altered Dap stability without interfering with the regulation of other $CRL4^{Cdt2}$ substrates. Using this strategy, we found that expressing a PIP-degron mutant Dap (Dap^{mDeg}) affects the *Drosophila* endocycle.

High-level overexpression of Dap was previously shown to induce precocious cell cycle exit (de Nooij et al., 1996; Lane et al., 1996). We were therefore initially surprised that expression of the Dap^{mDeg} mutant protein had no apparent effect on mitotic cycles in either the embryonic epidermis or wing imaginal disc. We could reproduce the precocious cell cycle arrest reported by Lane et al. (1996) using a *UASt-Dap* transgene, and our UASp transgenes were expressed at a lower level than with the UASt promoter. Thus, the level of Dap accumulation attained in our experiments reveals a difference between mitotic and endocycling cells. Such differences have been noted before. For example, Cyclin E expression is higher in mitotically dividing cells of the embryonic central nervous system than it is in endocycling cells (Richardson et al., 1993; Knoblich et al., 1994), probably as a result of E2f1-independent expression of *Cyclin E* (Duronio and O'Farrell, 1995). Thus, mitotic cycles might have higher Cyclin E-Cdk2 activity than endocycles, and as a result endocycles might be more sensitive to levels of Dap expression and thus require additional modes of Dap regulation. As with Dap, bypassing PIP degron-mediated destruction of E2f1 does not cause arrest of mitotically dividing cells, and S phase-coupled destruction of E2f1 plays an important role in the endocycle by helping generate oscillations of *Cyclin E* transcription (Shibutani et al., 2008; Zielke et al., 2011; Davidson and Duronio, 2012).

We make interpretations regarding the function of S phase-coupled Dap destruction in those tissues where Dap expression and Dap^{mDeg} expression have different effects. In this regard, our data provide evidence that S phase-coupled destruction of Dap has a modulatory role in endocycling cells, even in tissues such as the salivary gland where removal of Dap function does not prevent endocycle progression (Zielke et al., 2011). However, we note that our experiments do not directly address the role of PIP degron-mediated destruction of endogenous Dap. Addition of Dap to a mathematical model of the endocycle alters endocycle frequency, primarily by increasing the length between peaks of Cyclin E-Cdk2 activity, which we infer as a measure of G phase length. The model's predictions correspond with our results as well as previous data from ovarian follicle cells and nurse cells, where removal of *dap* results in decreased length of G phase and leads to endocycle defects (Hong et al., 2007). We propose that PIP degron-mediated destruction of Dap plays a role in modulating endocycle periodicity by depleting Dap protein during S phase, thereby lowering the threshold needed for Cyclin E-Cdk2 to drive S phase entry.

S phase-coupled destruction represents just one facet of Dap regulation in endocycling cells. Previous studies have shown that *dap* transcription is regulated by Cyclin E (de Nooij et al., 2000). Our data also suggest that PIP degron-mediated destruction is not the only regulator of Dap stability during S phase. We observed persistent fluctuations of Dap^{mDeg} protein accumulation that appear to be linked to the cell cycle, as Dap^{mDeg} levels were highest in G phase cells and tended to be lower in cells with the greatest levels of EdU incorporation. Any additional mode of Dap regulation is probably post-translational, as transgene transcription is controlled by the same GAL4 drivers and the transgenes include only a minimal 3′UTR. It has previously been shown that Dap protein stability is regulated by the $CRL1^{Skp2}$ ubiquitin ligase (also known

Development (2015) 142, 4288-4298 doi:10.1242/dev.115006

as SCF^{Skp2}) (Dui et al., 2013). $CRL1^{Skp2}$ activity is linked to the cell cycle, and mammalian p27 is targeted for destruction by $CRL1^{Skp2}$ following phosphorylation by Cyclin E-Cdk2 (Carrano et al., 1999; Sutterlüty et al., 1999; Tsvetkov et al., 1999; Nakayama and Nakayama, 2005). However, our data suggest that $CRL1^{Skp2}$ regulation of Dap might not be sufficient to control endocycle progression in the absence of PIP degron-mediated destruction. Multiple modes of regulation – PIP degron-dependent and independent destruction, as well as transcriptional regulation of *dap* by Cyclin E-Cdk2 – are probably required to cooperatively fine-tune Dap protein expression during the endocycle.

Finally, S phase destruction of CKIs might be a general feature of endocycle programs (Ullah et al., 2009a). $CRL4^{Cdt2}$ regulation of CKIs is required for trichome endocycles in *Arabidopsis* (Roodbarkelari et al., 2010). Similarly, $CRL1^{Skp2}$-mediated depletion of p57 (also known as CDKN1C) during S phase in endocycling trophoblast giant cells is crucial for endocycle progression (Hattori et al., 2000). Therefore, it is possible that some mode of S phase destruction of CKIs is a general feature of the endocycle program in most organisms.

MATERIALS AND METHODS

Generation of Dap transgenes

Wild-type or mutagenized (Stratagene) *dap* open reading frames were cloned into pENTR-d/TOPO (Invitrogen) before subcloning into either pHGW (*Drosophila* Gateway Vector Collection) for stable transfection of S2 cells (Davidson and Duronio, 2011) or a modified pPGW vector (a gift from Steve Rogers) that includes an AttB site for phiC31-mediated transgenesis.

Cell culture transfection, expression and analysis by flow cytometry

S2 cells collected 2-4 h after a 30 min, 37°C heat shock or dissociated wing disc samples were prepared for flow analysis as previously described (Davidson and Duronio, 2011). GFP expression and DNA content were measured using a Dako CyAn (S2 cells) or a Becton Dickinson LSR II (wing discs) flow cytometer and ModFit (S2 cells) or FlowJo (wing discs) software. Data from S2 analysis were analyzed for statistical significance with a two-way ANOVA test.

Fly stocks

UASp-GFP-Dap transgenes inserted into AttP2 [Bloomington Drosophila Stock Center (BDSC) #8622] were expressed using *Tub-GAL4/TM3* (BDSC #5138), *Ptc-GAL4* (BDSC #2017), and *c323-GAL4/CyO* (Manseau et al., 1997). UAS-GFP was obtained from the Bloomington Stock Center. UASt-DapII.2 was kindly provided by Christian Lehner.

Western blotting

Dechorionated embryos or salivary glands were lysed by disruption with a pestle in 2× lysis buffer (0.125M Tris pH 6.8, 1% SDS, 5% BME) and cleared twice by centrifugation. Samples were run on 4-15% Mini-PROTEAN TGX gels (BioRad), transferred to Immobilon-P PVDF membranes (Millipore), stained with 0.1% Ponceau in 5% acetic acid for 2 min, and imaged on a UVP Biospectrum Imaging System. Antibodies were: rabbit anti-Dap (1:1000; a gift from Christian Lehner), mouse anti-GFP (1:2000; JL-8, Clontech), mouse anti-lamin (1:1000; ADL84.12, DSHB), HRP-donkey anti-rabbit (1:30,000; catalog #NA934, GE Healthcare), and HRP-sheep anti-mouse (1:30,000; catalog #NA931, GE Healthcare). SuperSignal West Dura Chemiluminescent Substrate (Thermo) and Blue Devil Premium film were used to detect HRP activity (Genesee).

BrdU labeling, EdU labeling and immunofluorescence

BrdU labeling of embryos was performed as previously described (Sloan et al., 2012). For co-detection of S phase and Dap, embryos were fixed for 15 min in 3.7% formaldehyde after antibody staining prior to BrdU detection. Ovaries from 2- to 3-day-old females or third-instar larval wing discs were dissected in Grace's media, incubated for 1 h in 0.1 mg/ml EdU, and fixed for 20 min in 3.7% formaldehyde. EdU-labeled ovaries were fixed for 10 min in 3.7% formaldehyde after antibody staining, followed by EdU detection using the Click-iT EdU AlexaFluor 488 Imaging Kit (Invitrogen). Salivary glands were dissected from early third-instar larvae collected 96 h after egg deposition before undergoing EdU labeling, staining and detection as described for ovaries. Antibodies used were: rabbit anti-GFP (1:1000; catalog #ab290, Abcam), mouse anti-BrdU (1:500; catalog #347580, BD Biosciences), mouse anti-Dlg (1:1000; Hybridoma product number 4F3, DSHB), rat anti-Elav (1:100; Hybridoma product number 7E8A10, DSHB), rabbit anti-Dap (1:100, a gift from Christian Lehner), goat anti-rabbit AlexaFluor 488 (1:1000; catalog #A-11034, Invitrogen), and goat anti-mouse Cy3 (1:1000; catalog #115-165-003, Jackson Immunoresearch Laboratories). Imaging was carried out using a Zeiss 700 or Zeiss 710 confocal microscope and image processing was performed using Adobe Photoshop. Quantification of fluorescence was performed by measuring fluorescence intensity of single cells (delineated manually) using ImageJ (National Institutes of Health).

Quantification of S phase cell populations, cell density and salivary gland nuclear size

S phase was quantified in Stage 9 egg chambers in which follicle cell migration had progressed between 3/4 to 2/3 the length of the egg chamber. S phase percentage was calculated by counting all EdU-positive follicle cell nuclei in a single confocal section for 13 egg chambers. We similarly calculated the percentage of S phase cells in 18 salivary glands of each genotype dissected 96 h after egg deposition. For embryonic S phase analysis, we counted EdU-positive cell nuclei in single confocal sections of the anterior midguts of five to six Stage 13 embryos per genotype. We quantified cell density in the anterior midguts of five to six embryos per genotype by counting DAPI-positive nuclei within a defined region of a confocal section using ImageJ. Statistical significance was determined using two-sided *t*-tests. Nuclear area and DNA content of three DAPI-stained nuclei at the posterior end of five salivary glands from each genotype were measured using ImageJ. Data were normalized to the average nuclear area and average DAPI intensity of *ptc>GFP* nuclei and analyzed used two-sided *t*-tests. For DNA content the average cytoplasmic integrated density was subtracted from each measurement to control for background.

Mathematical modeling

We extended and revised the endocycle model of Zielke et al., (2011) to enhance the rate of Cyclin E deactivation through the addition of a Cyclin E-Dap-Cyclin E negative feedback loop (Fig. 6A). The revised model includes Cyclin E activation of Dap transcription (de Nooij et al., 2000), Dap inhibition of Cyclin E-Cdk2 activity, and $CRL4^{Cdt2}$ enhancement of Dap destruction. Using the previously described model convention, we defined the following differential equation to model the time-dependent DAP concentration:

$$\mathrm{DAP}'(t) = \mathrm{Ldap} + \frac{\mathrm{CYCE\,max\,D}\left(\frac{\mathrm{CYCE}(t)}{\mathrm{kCYCED}}\right)^{\mathrm{nuCD}}}{\left(\frac{\mathrm{CYCE}(t)}{\mathrm{kCYCED}}\right)^{\mathrm{nuCD}} + 1} - \frac{\mathrm{CUL\,max\,DAP} \times \mathrm{DAP}(t)\left(\frac{\mathrm{CUL}(t)}{\mathrm{kCULD}}\right)^{\mathrm{nuCD}}}{\left(\frac{\mathrm{CUL}(t)}{\mathrm{kCULD}}\right)^{\mathrm{nuCD}} + 1} - \frac{\mathrm{DAP}(t)}{\mathrm{HDAP}}, \quad (1)$$

where the first two terms on the right hand side of Eqn 1 account for exogenous and Cyclin E-dependent Dap expression, respectively, and the second two terms account for Cul4-dependent and basal Dap degradation, respectively. We modified the previously defined equation for Cyclin E levels (Equation 10 of Zielke et al., 2011) to include Dap-dependent

Development (2015) 142, 4288-4298 doi:10.1242/dev.115006

inhibition as follows:

$$\mathrm{CYCE}'(t) = \mathrm{Lcyce} \times \mathrm{delcyce}(t) - \frac{\mathrm{DAP\,max\,C} \times \mathrm{CYCE}(t)\left(\frac{\mathrm{DAP}(t)}{\mathrm{kDAPC}}\right)^{\mathrm{nuDC}}}{\left(\frac{\mathrm{DAP}(t)}{\mathrm{kDAPC}}\right)^{\mathrm{nuDC}} + 1} - \frac{\mathrm{CYCE}(t)}{\mathrm{HCYCE}}, \quad (2)$$

where the first term in Eqn 2 represents the synthesis of Cyclin E as a function of the previously defined delay cycle (Zielke et al., 2011), and the second and third terms define the rate of Dap induced and basal inhibition of Cyclin E, respectively. Starting from the values reported by Zielke et al. (2011), we performed a brute force parameter search to identify an appropriate set of model rate parameters such that the addition of endogenous Dap did not significantly alter the amplitude of Cyclin E from the previously established endocycle model (Table S1). Furthermore, we required that the removal of Dap mimic previously established *dap* mutant data (Zielke et al., 2011). We used the E2F spike duration as a proxy for G phase and the square pulse duration of the $CRL4^{Cdt2}$ as a proxy for the duration of S phase. Dap (1×) increased the duration of G phase by ∼1.2 times the length of G phase for the Dap-deficient mutant. For each subsequent multiplicative Dap addition (2×-10×) the length of G phase increased in proportion to 1.2× the previous G phase length.

Acknowledgements

We thank Christian Lehner (University of Zurich Institute of Molecular Life Sciences) and Steve Rogers (University of North Carolina Department of Biology) for reagents, Dan McKay for comments on the manuscript, the University of North Carolina (UNC) Flow Cytometry Core Facility, and Bob Bagnell of the UNC Microscopy Services Laboratory.

Competing interests

The authors declare no competing or financial interests.

Author contributions

C.I.S. and R.J.D. conceived of the study, analyzed the data, and prepared most of the manuscript. C.I.S. performed most *Drosophila* experiments with help from University of North Carolina at Chapel Hill undergraduates A.T. and T.M.; J.H.M. performed the wing disc flow analysis and western blotting. P.C.M. and T.C.E. revised the mathematical model of the endocycle, performed the modeling analysis, and prepared the figures and text for this portion of the manuscript.

Funding

The University of North Carolina (UNC) Flow Cytometry Core Facility and Microscopy Services Laboratory are supported in part by a National Cancer Institute Center Core Support Grant [CA016086] to the UNC Lineberger Comprehensive Cancer Center. This work was supported by a Seeding Postdoctoral Innovators in Research and Education (SPIRE) fellowship from National Institutes of Health (NIH) [K12 GM000678] to C.I.S., a Ruth L. Kirschstein National Research Service Award (NRSA) Predoctoral Fellowship from NIH [F31 AG044957] to J.H.M., an NRSA to Promote Diversity in Health-Related Research from NIH [F31 GM115224] and Initiative for Maximizing Student Diversity awards from NIH [R25 GM05533612; T32GM067553] to P.C.M., and NIH [R01 GM079271] to T.C.E. and [R01 GM57859 and R01 GM58921] to R.J.D. Deposited in PMC for release after 12 months.

Supplementary information

Supplementary information available online at
http://dev.biologists.org/lookup/suppl/doi:10.1242/dev.115006/-/DC1

References

Abbas, T. and Dutta, A. (2011). CRL4Cdt2: master coordinator of cell cycle progression and genome stability. *Cell Cycle* **10**, 241-249.
Abbas, T., Sivaprasad, U., Terai, K., Amador, V., Pagano, M. and Dutta, A. (2008). PCNA-dependent regulation of p21 ubiquitylation and degradation via the CRL4Cdt2 ubiquitin ligase complex. *Genes Dev.* **22**, 2496-2506.
Arias, E. E. and Walter, J. C. (2006). PCNA functions as a molecular platform to trigger Cdt1 destruction and prevent re-replication. *Nat. Cell Biol.* **8**, 84-90.
Arias, E. E. and Walter, J. C. (2007). Strength in numbers: preventing rereplication via multiple mechanisms in eukaryotic cells. *Genes Dev.* **21**, 497-518.
Bramsiepe, J., Wester, K., Weinl, C., Roodbarkelari, F., Kasili, R., Larkin, J. C., Hülskamp, M. and Schnittger, A. (2010). Endoreplication controls cell fate maintenance. *PLoS Genet.* **6**, e1000996.
Buttitta, L. A., Katzaroff, A. J., Perez, C. L., de la Cruz, A. and Edgar, B. A. (2007). A double-assurance mechanism controls cell cycle exit upon terminal differentiation in Drosophila. *Dev. Cell* **12**, 631-643.
Calvi, B. R., Lilly, M. A. and Spradling, A. C. (1998). Cell cycle control of chorion gene amplification. *Genes Dev.* **12**, 734-744.
Carrano, A. C., Eytan, E., Hershko, A. and Pagano, M. (1999). SKP2 is required for ubiquitin-mediated degradation of the CDK inhibitor p27. *Nat. Cell Biol.* **1**, 193-199.
Colonques, J., Ceron, J., Reichert, H. and Tejedor, F. J. (2011). A transient expression of Prospero promotes cell cycle exit of Drosophila postembryonic neurons through the regulation of Dacapo. *PLoS ONE* **6**, e19342.
Coward, J. and Harding, A. (2014). Size does matter: why polyploid tumor cells are critical drug targets in the war on cancer. *Front. Oncol.* **4**, 123.
Davidson, J. M. and Duronio, R. J. (2011). Using Drosophila S2 cells to measure S phase-coupled protein destruction via flow cytometry. *Methods Mol. Biol.* **782**, 205-219.
Davidson, J. M. and Duronio, R. J. (2012). S phase–coupled E2f1 destruction ensures homeostasis in proliferating tissues. *PLoS Genet.* **8**, e1002831.
Davoli, T. and de Lange, T. (2011). The causes and consequences of polyploidy in normal development and cancer. *Annu. Rev. Cell Dev. Biol.* **27**, 585-610.
de Nooij, J. C., Letendre, M. A. and Hariharan, I. K. (1996). A cyclin-dependent kinase inhibitor, Dacapo, is necessary for timely exit from the cell cycle during Drosophila embryogenesis. *Cell* **87**, 1237-1247.
de Nooij, J. C., Graber, K. H. and Hariharan, I. K. (2000). Expression of the cyclin-dependent kinase inhibitor Dacapo is regulated by cyclin E. *Mech. Dev.* **97**, 73-83.
De Veylder, L., Larkin, J. C. and Schnittger, A. (2011). Molecular control and function of endoreplication in development and physiology. *Trends Plant Sci.* **16**, 624-634.
Diffley, J. F. X. (2011). Quality control in the initiation of eukaryotic DNA replication. *Philos. Trans. R. Soc. B Biol. Sci.* **366**, 3545-3553.
Dui, W., Wei, B., He, F., Lu, W., Li, C., Liang, X., Ma, J. and Jiao, R. (2013). The Drosophila F-box protein dSkp2 regulates cell proliferation by targeting Dacapo for degradation. *Mol. Biol. Cell* **24**, 1676-1687.
Duronio, R. J. and O'Farrell, P. H. (1995). Developmental control of the G1 to S transition in Drosophila: cyclin E is a limiting downstream target of E2F. *Genes Dev.* **9**, 1456-1468.
Escudero, L. M. and Freeman, M. (2007). Mechanism of G1 arrest in the Drosophila eye imaginal disc. *BMC Dev. Biol.* **7**, 13.
Firth, L. C. and Baker, N. E. (2005). Extracellular signals responsible for spatially regulated proliferation in the differentiating Drosophila eye. *Dev. Cell* **8**, 541-551.
Follette, P. J., Duronio, R. J. and O'Farrell, P. H. (1998). Fluctuations in cyclin E levels are required for multiple rounds of endocycle S phase in Drosophila. *Curr. Biol.* **8**, 235-238.
Fox, D. T. and Duronio, R. J. (2013). Endoreplication and polyploidy: insights into development and disease. *Development* **140**, 3-12.
Gentric, G. and Desdouets, C. (2014). Polyploidization in liver tissue. *Am. J. Pathol.* **184**, 322-331.
Hattori, N., Davies, T. C., Anson-Cartwright, L. and Cross, J. C. (2000). Periodic expression of the cyclin-dependent kinase inhibitor p57(Kip2) in trophoblast giant cells defines a G2-like gap phase of the endocycle. *Mol. Biol. Cell* **11**, 1037-1045.
Havens, C. G. and Walter, J. C. (2009). Docking of a specialized PIP Box onto chromatin-bound PCNA creates a degron for the ubiquitin ligase CRL4Cdt2. *Mol. Cell* **35**, 93-104.
Havens, C. G. and Walter, J. C. (2011). Mechanism of CRL4(Cdt2), a PCNA-dependent E3 ubiquitin ligase. *Genes Dev.* **25**, 1568-1582.
Higa, L. A., Yang, X., Zheng, J., Banks, D., Wu, M., Ghosh, P., Sun, H. and Zhang, H. (2006). Involvement of CUL4 ubiquitin E3 ligases in regulating CDK inhibitors Dacapo/p27Kip1 and cyclin E degradation. *Cell Cycle* **5**, 71-77.
Hong, A., Lee-Kong, S., Iida, T., Sugimura, I. and Lilly, M. A. (2003). The p27cip/kip ortholog dacapo maintains the Drosophila oocyte in prophase of meiosis I. *Development* **130**, 1235-1242.
Hong, A., Narbonne-Reveau, K., Riesgo-Escovar, J., Fu, H., Aladjem, M. I. and Lilly, M. A. (2007). The cyclin-dependent kinase inhibitor Dacapo promotes replication licensing during Drosophila endocycles. *EMBO J.* **26**, 2071-2082.
Hu, J. and Xiong, Y. (2006). An evolutionarily conserved function of proliferating cell nuclear antigen for Cdt1 degradation by the Cul4-Ddb1 ubiquitin ligase in response to DNA damage. *J. Biol. Chem.* **281**, 3753-3756.
Hu, J., McCall, C. M., Ohta, T. and Xiong, Y. (2004). Targeted ubiquitination of CDT1 by the DDB1–CUL4A–ROC1 ligase in response to DNA damage. *Nat. Cell Biol.* **6**, 1003-1009.
Kim, J., Feng, H. and Kipreos, E. T. (2007). C. elegans CUL-4 prevents rereplication by promoting the nuclear export of CDC-6 via a CKI-1-dependent pathway. *Curr. Biol.* **17**, 966-972.
Kim, Y., Starostina, N. G. and Kipreos, E. T. (2008). The CRL4Cdt2 ubiquitin ligase targets the degradation of p21Cip1 to control replication licensing. *Genes Dev.* **22**, 2507-2519.

Development (2015) 142, 4288-4298 doi:10.1242/dev.115006

Kim, D. H., Budhavarapu, V. N., Herrera, C. R., Nam, H. W., Kim, Y. S. and Yew, P. R. (2010). The CRL4Cdt2 ubiquitin ligase mediates the proteolysis of cyclin-dependent kinase inhibitor Xic1 through a direct association with PCNA. *Mol. Cell. Biol.* **30**, 4120-4133.

Knoblich, J. A., Sauer, K., Jones, L., Richardson, H., Saint, R. and Lehner, C. F. (1994). Cyclin E controls S phase progression and its down-regulation during Drosophila embryogenesis is required for the arrest of cell proliferation. *Cell* **77**, 107-120.

Lane, M. E., Sauer, K., Wallace, K., Jan, Y. N., Lehner, C. F. and Vaessin, H. (1996). Dacapo, a cyclin-dependent kinase inhibitor, stops cell proliferation during Drosophila development. *Cell* **87**, 1225-1235.

Lee, H. O., Davidson, J. M. and Duronio, R. J. (2009). Endoreplication: polyploidy with purpose. *Genes Dev.* **23**, 2461-2477.

Lilly, M. A. and Duronio, R. J. (2005). New insights into cell cycle control from the Drosophila endocycle. *Oncogene* **24**, 2765-2775.

Manseau, L., Baradaran, A., Brower, D., Budhu, A., Elefant, F., Phan, H., Philp, A. V., Yang, M., Glover, D., Kaiser, K. et al. (1997). GAL4 enhancer traps expressed in the embryo, larval brain, imaginal discs, and ovary of Drosophila. *Dev. Dyn.* **209**, 310-322.

Mehrotra, S., Maqbool, S. B., Kolpakas, A., Murnen, K. and Calvi, B. R. (2008). Endocycling cells do not apoptose in response to DNA rereplication genotoxic stress. *Genes Dev.* **22**, 3158-3171.

Moberg, K. H., Bell, D. W., Wahrer, D. C. R., Haber, D. A. and Hariharan, I. K. (2001). Archipelago regulates Cyclin E levels in Drosophila and is mutated in human cancer cell lines. *Nature* **413**, 311-316.

Nakayama, K. I. and Nakayama, K. (2005). Regulation of the cell cycle by SCF-type ubiquitin ligases. *Semin. Cell Dev. Biol.* **16**, 323-333.

Nishitani, H., Shiomi, Y., Iida, H., Michishita, M., Takami, T. and Tsurimoto, T. (2008). CDK inhibitor p21 is degraded by a proliferating cell nuclear antigen-coupled Cul4-DDB1Cdt2 pathway during S phase and after UV irradiation. *J. Biol. Chem.* **283**, 29045-29052.

Nordman, J. and Orr-Weaver, T. L. (2012). Regulation of DNA replication during development. *Development* **139**, 455-464.

Raslova, H., Kauffmann, A., Sekkai, D., Ripoche, H., Larbret, F., Robert, T., Le Roux, D. T., Kroemer, G., Debili, N., Dessen, P. et al. (2007). Interrelation between polyploidization and megakaryocyte differentiation: a gene profiling approach. *Blood* **109**, 3225-3234.

Richardson, H. E., O'Keefe, L. V., Reed, S. I. and Saint, R. (1993). A Drosophila G1-specific cyclin E homolog exhibits different modes of expression during embryogenesis. *Development* **119**, 673-690.

Roodbarkelari, F., Bramsiepe, J., Weinl, C., Marquardt, S., Novak, B., Jakoby, M. J., Lechner, E., Genschik, P. and Schnittger, A. (2010). Cullin 4-ring finger-ligase plays a key role in the control of endoreplication cycles in Arabidopsis trichomes. *Proc. Natl. Acad. Sci. USA* **107**, 15275-15280.

Senga, T., Sivaprasad, U., Zhu, W., Park, J. H., Arias, E. E., Walter, J. C. and Dutta, A. (2006). PCNA is a cofactor for Cdt1 degradation by CUL4/DDB1-mediated N-terminal ubiquitination. *J. Biol. Chem.* **281**, 6246-6252.

Shcherbata, H. R., Althauser, C., Findley, S. D. and Ruohola-Baker, H. (2004). The mitotic-to-endocycle switch in Drosophila follicle cells is executed by Notch-dependent regulation of G1/S, G2/M and M/G1 cell-cycle transitions. *Development* **131**, 3169-3181.

Shibutani, S. T., de la Cruz, A. F., Tran, V., Turbyfill, W. J., III, Reis, T., Edgar, B. A. and Duronio, R. J. (2008). Intrinsic negative cell cycle regulation provided by PIP box- and Cul4Cdt2-mediated destruction of E2f1 during S phase. *Dev. Cell* **15**, 890-900.

Sloan, R. S., Swanson, C. I., Gavilano, L., Smith, K. N., Malek, P. Y., Snow-Smith, M., Duronio, R. J. and Key, S. C. (2012). Characterization of null and hypomorphic alleles of the Drosophila l(2)dtl/cdt2 gene: Larval lethality and male fertility. *Fly* **6**, 173-183.

Storchova, Z. and Pellman, D. (2004). From polyploidy to aneuploidy, genome instability and cancer. *Nat. Rev. Mol. Cell Biol.* **5**, 45-54.

Sukhanova, M. J. and Du, W. (2008). Control of cell cycle entry and exiting from the second mitotic wave in the Drosophila developing eye. *BMC Dev. Biol.* **8**, 7.

Sutterlüty, H., Chatelain, E., Marti, A., Wirbelauer, C., Senften, M., Müller, U. and Krek, W. (1999). p45SKP2 promotes p27Kip1 degradation and induces S phase in quiescent cells. *Nat. Cell Biol.* **1**, 207-214.

Tsvetkov, L. M., Yeh, K.-H., Lee, S.-J., Sun, H. and Zhang, H. (1999). p27(Kip1) ubiquitination and degradation is regulated by the SCF(Skp2) complex through phosphorylated Thr187 in p27. *Curr. Biol.* **9**, 661-664.

Ullah, Z., Kohn, M. J., Yagi, R., Vassilev, L. T. and DePamphilis, M. L. (2008). Differentiation of trophoblast stem cells into giant cells is triggered by p57/Kip2 inhibition of CDK1 activity. *Genes Dev.* **22**, 3024-3036.

Ullah, Z., Lee, C. Y. and DePamphilis, M. L. (2009a). Cip/Kip cyclin-dependent protein kinase inhibitors and the road to polyploidy. *Cell Div.* **4**, 10.

Ullah, Z., Lee, C. Y., Lilly, M. A. and DePamphilis, M. L. (2009b). Developmentally programmed endoreduplication in animals. *Cell Cycle* **8**, 1501-1509.

Unhavaithaya, Y. and Orr-Weaver, T. L. (2012). Polyploidization of glia in neural development links tissue growth to blood-brain barrier integrity. *Genes Dev.* **26**, 31-36.

Vidwans, S. J. and Su, T. T. (2001). Cycling through development in Drosophila and other metazoa. *Nat. Cell Biol.* **3**, E35-E39.

Weiss, A., Herzig, A., Jacobs, H. and Lehner, C. F. (1998). Continuous Cyclin E expression inhibits progression through endoreduplication cycles in Drosophila. *Curr. Biol.* **8**, 239-242.

Zielke, N., Kim, K. J., Tran, V., Shibutani, S. T., Bravo, M.-J., Nagarajan, S., van Straaten, M., Woods, B., von Dassow, G., Rottig, C. et al. (2011). Control of Drosophila endocycles by E2F and CRL4(CDT2). *Nature* **480**, 123-127.

Zielke, N., Edgar, B. A. and DePamphilis, M. L. (2013). Endoreplication. *Cold Spring Harb. Perspect. Biol.* **5**, a012948.